Progress In Electromagnetics Research Letters, Vol. 85, 1–8, 2019

Simplified Analysis of Symmetrical RF Crossovers Extended with Arbitrary Complex Passive Two-Port Networks

Mohammad A. Maktoomi[1, *], Mohammad H. Maktoomi[2], Zeba N. Zafar[1], Mohamed Helaoui[3], and Fadhel M. Ghannouchi[3]

Abstract—There are three mathematical conditions that must be solved simultaneously for the analysis of a fully-symmetric radio-frequency (RF) crossover. When additional reciprocal two-port networks — which might be of an arbitrarily high complexity — are appended at each port of a crossover, analysis of the modified crossover becomes very tedious. Therefore, this paper examines the requirement of the three conditions in such scenario. We show that two of the three conditions can be invoked without considering the additional two-port networks altogether. This is a remarkable simplification considering that the additional two-port networks, in general, would necessitate dealing with more involved algebraic calculations. To demonstrate the usefulness of the presented theory, for the first time, analysis and design of a dual-frequency port-extended crossover is included. A prototype of the dual-frequency crossover operating concurrently at 1 GHz and 2 GHz is manufactured on a Rogers RO4350B laminate having 30 mil substrate height and 3.66 dielectric constant. The close resemblance between the EM simulated and measured results validates the analytical equations.

1. INTRODUCTION

A Crossover is a matched 4-port passive device. This device allows two signals to cross each other, ideally, with infinite isolation. When the two signals are to cross each other, an air-bridge or an underpass could be used for this purpose. But, a microstrip crossover is a planar solution that is easier to fabricate and incur a reduced cost [1, 2]. This component has become very significant considering its potential application in a Butler matrix utilized in antenna beamforming for the upcoming 5G wireless communication technologies [3]. In view of the recent trends in multi-band components [4–6], there is a renewed interest in the analysis and design of dual-frequency crossovers [2, 3, 7, 8]. On the other hand, utilization of additional two-port network dates to 1976, when it was first reported as a methodology to enhance bandwidth of the conventional directional coupler [8]. Later, its application was shown in achieving dual-frequency behavior in coupler and power dividers [9, 10]. Despite many recent interesting attempts leading to realization of multiple channels and wideband crossovers [11–13], the port-extension technique could not get attention in the case of crossovers. A relatively more complex structure of a crossover is a hindrance to any such effort. Therefore, this paper presents a technique leading to a much more simplified analysis of port-extended crossovers formulated in the form of a general rule. This rule is further invoked in the analysis of a new dual-frequency crossover employing a transmission-line section as a port-extension network.

The remainder of this paper is organized as follows. The basic mathematical conditions that are required to be solved simultaneously for the analysis of crossovers are reviewed in Section 2. In addition, a new theory is presented for the port-extended crossovers leading to the simplified analysis rule. Application of the proposed rule is demonstrated in Section 3, whereas the developed prototype as well as the simulated and measurement results are discussed in Section 4. Finally, conclusions are presented in Section 5.

Received 18 March 2019, Accepted 22 May 2019, Scheduled 9 June 2019

* Corresponding author: Mohammad A. Maktoomi (mohammad.maktoomi@scranton.edu).

[1] University of Scranton, Scranton, USA. [2] Washington State University, Vancouver, USA. [3] University of Calgary, Calgary, Canada.

2. CROSSOVERS AND THEIR SIMPLIFIED ANALYSIS

The black-box diagram of a fully-symmetric crossover is depicted in Fig. 1. Being fully-symmetric simply mean that the crossover would appear the same if one looks into any one of the four ports as the input port. This crossover serves as a core structure in the proposed port-extended crossover in the following subsection. An ideal crossover is governed by the following S-parameters [1]:

$$S_{11} = S_{21} = S_{41} = 0, \quad |S_{31}| = 1. \tag{1}$$

Equation (1) means that if one injects some power into port 1, none of it goes to port 2 — all the power gets cross coupled into port 3, whereas port 4 is an isolated port. Owing to the presence of full symmetry the even-odd mode analysis method can be invoked in Fig. 1, which results into four eigen-admittances Y_{ij}, namely, Y_{ee}, Y_{eo}, Y_{oe}, and Y_{oo}. These eigen-admittances are related with the S-parameters as follows [14]:

$$S_{11} = \frac{\Gamma_{ee} + \Gamma_{eo} + \Gamma_{oe} + \Gamma_{oo}}{4} \tag{2}$$

$$S_{21} = \frac{\Gamma_{ee} - \Gamma_{eo} + \Gamma_{oe} - \Gamma_{oo}}{4} \tag{3}$$

$$S_{31} = \frac{\Gamma_{ee} - \Gamma_{eo} - \Gamma_{oe} + \Gamma_{oo}}{4} \tag{4}$$

$$S_{41} = \frac{\Gamma_{ee} + \Gamma_{eo} - \Gamma_{oe} - \Gamma_{oo}}{4} \tag{5}$$

where,

$$\Gamma_{ij} = \frac{1 - Z_0 Y_{ij}}{1 + Z_0 Y_{ij}}, \quad i = \{e, o\}, \quad j = \{e, o\} \tag{6}$$

and Z_0 is the port-termination impedance.

Using Eqs. (2)–(6) into Eq. (1) and after doing some algebraic manipulations, the following three expressions that we call *Condition* 1, *Condition* 2, and *Condition* 3, are achieved [2]:

$$Condition1: \; Y_{ee} = Y_{oo} \tag{7}$$

$$Condition2: \; Y_{eo} = Y_{oe} \tag{8}$$

$$Condition3: \; Y_{ee}Y_{eo} = 1/Z_0^2. \tag{9}$$

In any fully-symmetric crossover, these three conditions must be applied to derive their design equations. For sake of brevity, we define: $Y_{ee} = jr_1$, $Y_{eo} = jr_2$, $Y_{oe} = jr_3$, and $Y_{oo} = jr_4$.

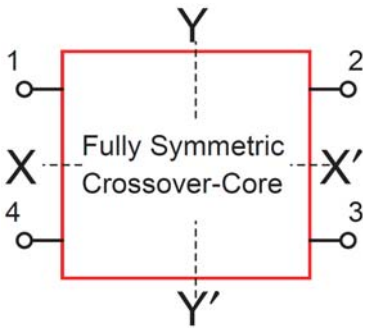

Figure 1. Black box diagram of a fully-symmetric crossover-core. XX' and YY' are the two axes of symmetry.

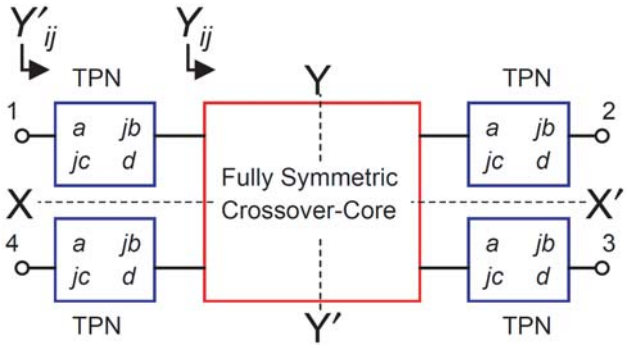

Figure 2. Black-box diagram of a port-extended crossover. Additional two-port networks are appended at each port of the crossover-core to get a port-extended crossover. TPN: two-port network.

2.1. Analysis of Crossover with Additional Passive Two-Port Networks

The modified crossover shown in Fig. 2 is obtained from the original crossover by appending identical reciprocal two-port networks at each port. It is apparent that this modification does not alter the full-symmetry defined in the preceding subsection. And therefore, the even-odd mode analysis can still be applied. The eigen-admittances of the modified crossover are denoted with primed notations, that is, as Y'_{ij}. Now, it is well known that the input admittance, Y_{in}, of a two-port network terminated with a load admittance, Y_L, in terms of the ABCD parameters is given as follows:

$$Y_{in} = \frac{DY_L + C}{BY_L + A} \tag{10}$$

The modified eigen-admittances, Y'_{ij}, valid for Fig. 2 can be evaluated using Eq. (10) by recognizing that $A = a$, $B = jb$, $C = jc$, and $D = d$, and the fact that $Y_{ij} = jr_k$, $k = \{1, 2, 3, 4\}$ will replace Y_L in Eq. (10):

$$Y'_{ee} = \frac{j(c + dr_1)}{(a - br_1)} \tag{11}$$

$$Y'_{eo} = \frac{j(c + dr_2)}{(a - br_2)} \tag{12}$$

$$Y'_{oe} = \frac{j(c + dr_3)}{(a - br_3)} \tag{13}$$

$$Y'_{oo} = \frac{j(c + dr_4)}{(a - br_4)} \tag{14}$$

Now, *Condition* 1 is invoked in the modified Crossover as follows:

$$Y'_{ee} = Y'_{oo} \tag{15}$$

which is further simplified using Eqs. (11) and (14) as:

$$c = \frac{ad(r_4 - r_1)}{b(r_1 - r_4)} \tag{16}$$

If $r_1 - r_4 \neq 0$, then from Eq. (16):

$$c = \frac{-ad}{b} \tag{17}$$

However, recognizing that $ad + bc = 1$ for the considered reciprocal two-port networks and substituting $ad = 1 - bc$ in the right-hand side of Eq. (17) does not yield any meaningful result, therefore, we must conclude that indeed $r_1 - r_4 = 0$, that is:

$$r_1 = r_4 \tag{18}$$

$$\Rightarrow\ jr_1 = jr_4\ \Rightarrow\ Y_{ee} = Y_{oo} \tag{19}$$

Equation (19) is a very interesting result: we started with $Y'_{ee} = Y'_{oo}$ in Eq. (15) and despite the presence of extra two-port networks, it led us to Eq. (19): $Y_{ee} = Y_{oo}$, that is, while invoking *Condition* 1 the two-port networks can be omitted altogether.

Similarly, the following result is obtained upon application of *Condition* 2, namely $Y'_{eo} = Y'_{oe}$ in Fig. 2:

$$r_2 = r_3 \tag{20}$$

$$\Rightarrow\ jr_1 = jr_4\ \Rightarrow\ Y_{eo} = Y_{oe} \tag{21}$$

That is, again, while invoking *Condition* 2 the two-port networks can be omitted altogether. Thus, based on Eqs. (19) and (21) we can state a general rule for the analysis of any fully-symmetric crossover with extra arbitrarily complex identical reciprocal two-port networks:

"Invoking conditions 1 and 2 in the modified Crossover is equivalent to their applications without considering the additional two-port network altogether."

In addition, the following simplified equation is obtained for the modified crossover upon application of *Condition* 3, $Y'_{ee}Y'_{eo} = 1/Z_0^2$:

$$(b^2 + d^2Z_0^2)r_1r_2 + (cdZ_0^2 - ab)(r_1 + r_2) + (a^2 + c^2Z_0^2) = 0 \tag{22}$$

3. APPLICATION: A NOVEL PORT-EXTENDED DUAL-FREQUENCY CROSSOVER

To show application of the simplified analysis rule presented in the previous Section, the proposed dual-frequency crossover shown in Fig. 3 is considered. It is composed of a crossover-core structure (drawn in blue color in the online version of this paper) that is shown inside the dotted region. The extra transmission lines having characteristic impedance Z_x and electrical length θ serve as additional two-port networks. To analyze the proposed crossover using the developed simplified analysis rule, we proceed as follows:

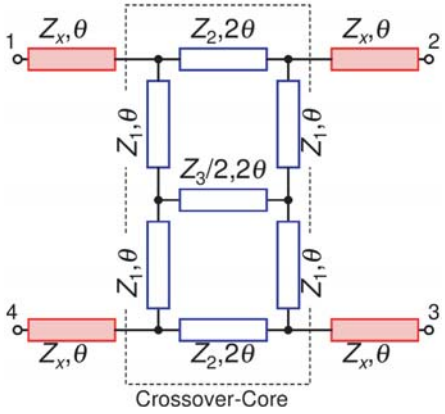

Figure 3. Proposed port-extended dual-frequency crossover. The crossover-core is shown inside the dotted box whereas the shaded transmission-lines serves as the additional two-port networks.

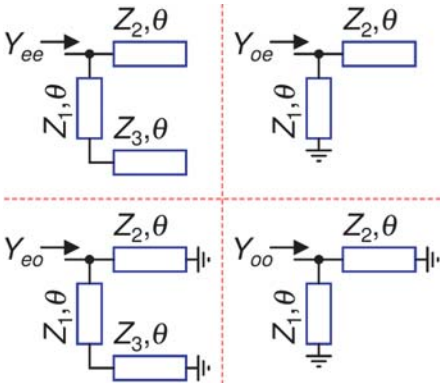

Figure 4. The even-odd mode equivalent circuits of the crossover-core obtained by omitting the port-extension transmission lines shown in Fig. 3.

Step 1. Omit the additional two-port networks and find the even-odd mode eigen-admittances of the resulting crossover-core:

The even-odd mode equivalent circuits are shown in Fig. 4, and the corresponding eigen-admittances are found as follows.

$$Y_{ee} = j\frac{\tan\theta}{Z_2} + j\frac{(Z_1+Z_3)\tan\theta}{Z_1(Z_3 - Z_1\tan^2\theta)} = jr_1 \tag{23}$$

$$Y_{eo} = -j\frac{\cot\theta}{Z_2} + j\frac{(Z_3\tan\theta - Z_1\cot\theta)}{Z_1(Z_1+Z_3)} = jr_2 \tag{24}$$

$$Y_{oe} = -j\frac{-\cot\theta}{Z_1} + j\frac{\tan\theta}{Z_2} = jr_3 \tag{25}$$

$$Y_{oo} = -j\frac{-\cot\theta}{Z_1} - j\frac{\cot\theta}{Z_2} = jr_4 \tag{26}$$

Step 2. Invoke *Conditions* 1 and 2 given by Eqs. (7) and (8):

First, Z_2 is found by invoking $Y_{eo} = Y_{oe}$:

$$Z_2 = \frac{Z_1(Z_1+Z_3)}{Z_3} \tag{27}$$

Subsequently, Z_3 is found by enforcing $Y_{ee} = Y_{oo}$:

$$Z_3 = -\frac{Z_1\cos 2\theta}{2\cos^2\theta} \tag{28}$$

By substituting Z_3 from Eq. (28) into Eq. (27), we get:

$$Z_2 = -\frac{Z_1}{\cos 2\theta} \tag{29}$$

Step 3. Use Eq. (22) to obtain the final design equations:

To apply Eq. (22), first r_1+r_2 and r_1r_2 are found using Eqs. (23)–(26) along with Eqs. (28) and (29):

$$r_1 + r_2 = \frac{k_1}{Z_1} \tag{30}$$

$$r_1 r_2 = \frac{k_2}{Z_1^2} \tag{31}$$

where,

$$k_1 = -(\cot\theta + \tan\theta(1 + 2\cos 2\theta)) \tag{32}$$

$$k_2 = (1 + \cos 2\theta)(1 + \tan^2\theta \cos 2\theta) \tag{33}$$

Then, by substituting Eqs. (30) and (31) into Eq. (22), we get:

$$Z_1 = \frac{-B \pm \sqrt{B^2 - 4AC}}{2A} \tag{34}$$

where,

$$A = a^2 + c^2 Z_0^2 \tag{35}$$

$$B = k_1(cdZ_0^2 - ab) \tag{36}$$

$$C = k_2(b^2 + d^2 Z_0^2) \tag{37}$$

where, $a = \cos\theta$, $b = Z_x \sin\theta$, $c = \sin\theta/Z_x$, and $d = \cos\theta$. In Eq. (34), any negative or a physically unrealizable value of Z_1 must be discarded. The chosen value of Z_1 upon evaluation from (34) is further utilized to find Z_3 and Z_2 using Eqs. (28)–(29). Z_x is a free variable that can be chosen to be anywhere between 20 Ω to 120 Ω for a microstrip implementation. It may be noted that for a dual-frequency operation, θ is evaluated using the following expression [2]:

$$\theta = \frac{m\pi}{1+r}, \quad r = f_2/f_1, \quad m: \text{ integer} \geq 1. \tag{38}$$

4. SIMULATION, PROTOTYPE, AND MEASUREMENT RESULTS

To assess the frequency-ratio achievable in the proposed crossover, the variation of various line-impedances is plotted in Fig. 5 using the design equations deduced in the previous section. It must be noted Z_x is assumed an independent variable and for each value of frequency-ratio, it is chosen such that one gets physically realizable values of Z_1, Z_2, and Z_3. It is apparent from the result shown in Fig. 5 that achievable frequency-ratio is from 1.3 to 2 considering that the characteristic impedances are limited between 20 Ω to 120 Ω. In contrast, a conventional double-box crossover can operate for a frequency-ratio lying between 1.5 to 1.9 [Figs. 2, 3]. Since Z_x is a free variable, Fig. 5 represents

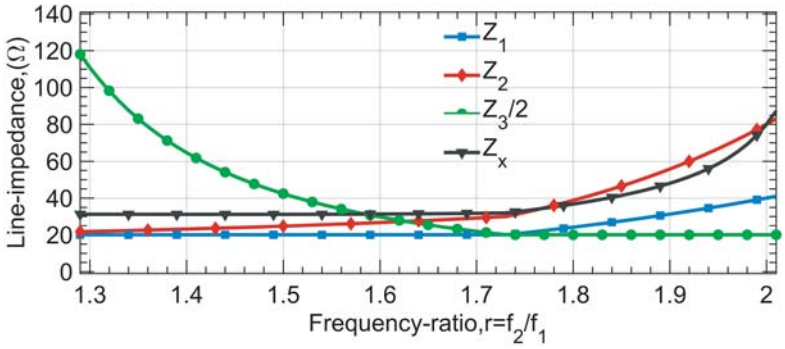

Figure 5. The line-impedance vs frequency-ratio plot of the proposed port-extended dual-frequency crossover assuming available characteristic impedance in the range [20 Ω, 120 Ω].

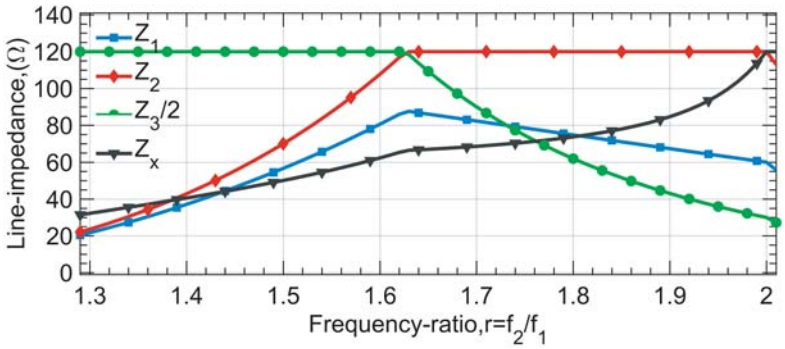

Figure 6. The line-impedance vs frequency-ratio plot of the proposed port-extended dual-frequency crossover allowing Z_x to assume another set of values.

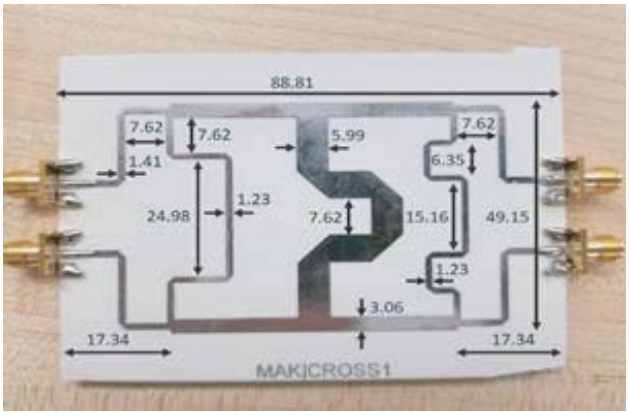

Figure 7. Layout the proposed port-extended dual-frequency crossover. The dimensions are in mm.

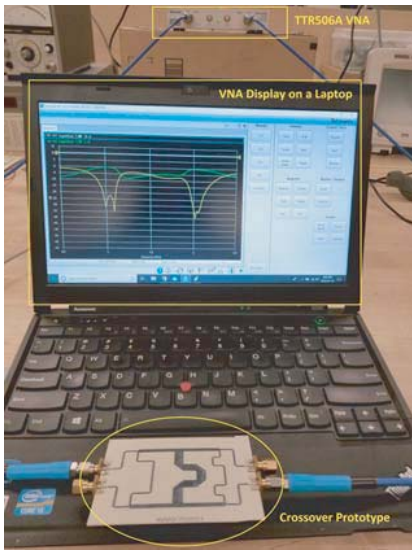

Figure 8. The measurement setup for the S-parameter of the fabricated prototype using a TTR506A VNA. The plots being shown on the laptop screen are $|S_{11}|$ (yellow) and $|S_{31}|$ (green).

just one of the many possible impedance variation profiles. For example, Fig. 6 shows another possible line-impedance variation obtained by forcing Z_x to take another set of values.

For validation of the theory, a prototype operating concurrently at 1 GHz and 2 GHz is designed, fabricated, and measured. A Rogers RO4350B substrate having a dielectric constant $\epsilon_r = 3.66$, dissipation factor $\tan\delta = 0.003$, substrate height = 0.762 mm, and copper cladding of 35 µm on both the sides is used. Values of various transmission line parameters are as follows: $Z_x = 80\,\Omega$, $Z_1 = 40\,\Omega$, $Z_2 = 80\,\Omega$, $Z_3 = 40\,\Omega$, and $\theta = 60°$. The Keysight ADS software was used for the design and during the preparation of this writing some simulations were also carried out using NI AWRDE. The fabricated prototype is depicted in Fig. 7 along with the dimensions of various transmission line elements annotated in mm. It must be noted that due to the presence of several T-junctions and bends in structure, the final microstrip structure needed fine tuning using the optimization feature of ADS. The S-parameters of the prototype were measured using a Tektronix TTR506A vector network analyzer (VNA) as shown in Fig. 8 with its IF bandwidth set at 1 kHz. The electromagnetic simulation (EM) and the measured results are compared in Fig. 9. The measured device shows that its return loss and isolations are 20 dB or better. Furthermore, for a 15-dB reference point the return loss bandwidths are 175 MHz at f_1 and 195 MHz at f_2, and the isolation bandwidths are 260 MHz at f_1 and 100 MHz at f_2. These are adequate

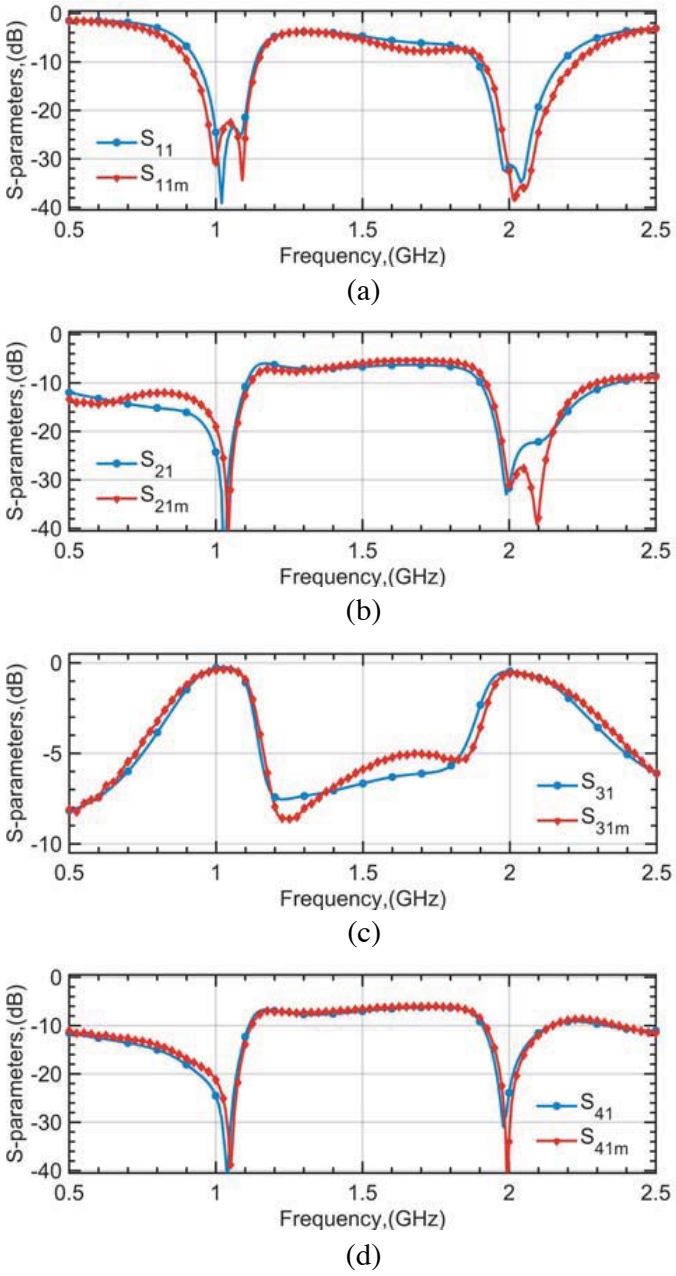

Figure 9. Comparison of EM simulated (without a subscript m) and measured (shown with subscript m) S-parameters magnitude in dB (a) $|S_{11}|$, (b) $|S_{21}|$, (c) $|S_{31}|$, and (d) $|S_{41}|$.

bandwidth for dual-frequency applications. Moreover, the measured insertion losses $|S_{31}|$ are -0.4 dB at f_1 and -0.58 dB at f_2, respectively. The corresponding EM simulated values of $|S_{31}|$ are -0.27 dB at f_1 and -0.48 dB at f_2. It is apparent that there is an excellent resemblance between the EM simulated and measurement results.

5. CONCLUSION

To perform analysis of a fully-symmetric crossover with extended two-port networks at each port is a very tedious task. This paper presents a rule that greatly helps simplify the analysis of such fully-symmetric crossovers. Thorough analysis was conducted to show that two of the required conditions

for the analysis of the crossover could be applied without considering the additional two-port networks altogether. The derived rule was invoked during the analysis of the proposed dual-frequency crossover, which helped us quickly get the design equations. The EM simulated and measured S-parameters of the designed prototype match well with each other and hence validate the theory presented in this paper.

ACKNOWLEDGMENT

Mohammad A. Maktoomi would like to acknowledge the generous support from the National Instruments through its NI AWR university partnership program and Rogers corporation for providing PCB laminates. He also appreciates much help from the Academic Dean of the College of Arts and Sciences at the University of Scranton, Dr. Brian Conniff and Chairperson of the Physics and Electrical Engineering department, Dr. Andrew Berger for providing internal grants to facilitate the measurement.

REFERENCES

1. Wight, J. S., W. J. Chudobiak, and V. Makios, "A microstrip and stripline crossover structure (letters)," *IEEE Trans. Microw. Theory Techn.*, Vol. 24, No. 5, 270–270, May 1976.
2. Lin, F., Q. Chu, and S. W. Wong, "Dual-band planar crossover with two-section branch-line structure," *IEEE Trans. Microw. Theory Techn.*, Vol. 61, No. 6, 2309–2316, Jun. 2013.
3. Ren, H., M. Zhou, H. Zhang, and B. Arigong, "A novel dual-band zero-phase true crossover with arbitrary port impedance," *IEEE Microw. Wireless Compon. Lett.*, Vol. 29, No. 1, 29–31, Jan. 2019.
4. Feng, W., Y. Zhao, W. Che, R. Gómez-García, and Q. Xue, "Multi-band balanced couplers with broadband common-mode suppression," *IEEE Trans. Circuits Syst. II, Exp. Briefs*, Vol. 65, No. 12, 1964–1968, Dec. 2018.
5. Feng, W., Y. Zhao, W. Che, H. Chen, and W. Yang, "Dual-/tri-band branch line couplers with high power division isolation using coupled lines," *IEEE Trans. Circuits Syst. II, Exp. Briefs*, Vol. 65, No. 4, 461–465, Apr. 2018.
6. Gómez-García, R., R. Loeches-Sanchez, D. Psychogiou, and D. Peroulis, "Multi-stub-loaded differential-mode planar multiband bandpass filters," *IEEE Trans. Circuits Syst. II, Exp. Briefs*, Vol. 65, No. 3, 271–275, Mar. 2018.
7. Wong, F. L. and K. K. M. Cheng, "A novel, planar, and compact crossover design for dual-band applications," *IEEE Trans. Microw. Theory Techn.*, Vol. 59, No. 3, 568–573, Mar. 2011.
8. Zhao, Y., W. Feng, T. Zhang, W. Che, and Q. Xue, "Planar single/dual-band crossovers with large-frequency ratios using coupled lines," *IEEE Microw. Wireless Compon. Lett.*, Vol. 27, No. 10, 870–872, Oct. 2017.
9. Kim, H., B. Lee, and M. J. Park, "Dual-band branch-line coupler with port extensions," *IEEE Trans. Microw. Theory Techn.*, Vol. 58, No. 3, 651–655, Mar. 2010.
10. Chu, Q., F. Lin, Z. Lin, and Z. Gong, "Novel design method of tri-band power divider," *IEEE Trans. Microw. Theory Techn.*, Vol. 59, No. 9, 2221–2226, Sep. 2011.
11. Chu, P. and C. Tang, "Design of a compact planar crossover with four intersecting channels," *IEEE Microw. Wireless Compon. Lett.*, Vol. 28, No. 4, 293–295, Apr. 2018.
12. Wang, Y., E. Oliver, N. Nguyen-Trong, J. Ness, and A. M. Abbosh, "Hyperwideband microwave crossover using bridged suspended substrate line configuration," *IEEE Microw. Wireless Compon. Lett.*, Vol. 28, No. 12, 1083–1085, Dec. 2018.
13. Jiao, L., et al., "A wideband uniplanar double-ring crossover with balanced and single-ended paths," *IEEE Trans. Microw. Theory Techn.*, Vol. 66, No. 12, 5238–5247, Dec. 2018.
14. Collin, R. E., *Foundations for Microwave Engineering*, 2nd Edition, Wiley-IEEE Press, USA, Jan. 2001.